Spin polarization of carriers in InGaAs self-assembled quantum rings inserted in GaAs-AlGaAs resonant tunneling devices

V. Orsi Gordo[1], Y. Galvão Gobato[1,5], H.V.A. Galeti[2], M.J.S.P. Brasil[3], D. Taylor[4], M. Henini[4]

1.-Departamento de Física, Universidade Federal de São Carlos 13565-905, São Carlos, SP, Brazil

2.-Departamento de Engenharia Elétrica, Universidade Federal de São Carlos 13565-905, São Carlos, SP, Brazil

3.-Instituto de Física “Gleb Wataghin”, Universidade Estadual de Campinas-UNICAMP, 13083-970, Campinas, SP, Brazil

4.-School of Physics and Astronomy, Nottingham Nanotechnology and Nanoscience Centre, University of Nottingham, Nottingham NG7 2RD, UK

5.-yara.ufscar@gmail.com

In this work, we have investigated transport and polarization resolved photoluminescence (PL) of n-type GaAs-AlGaAs resonant tunneling diodes (RTDs) containing a layer of InGaAs self-assembled quantum rings (QRs) in the quantum well (QW). All measurements were performed under applied voltage, magnetic fields up to 15 T and using linearly polarized laser excitation. It was observed that the QRs’ PL intensity and the circular polarization degree (CPD) oscillate periodically with applied voltage under high magnetic fields at 2 K. Our results demonstrate an effective voltage control of the optical and spin properties of InGaAs QRs inserted into RTDs.

Keywords: quantum rings, photoluminescence, spin polarization, resonant tunneling

INTRODUCTION

Quantum rings (QRs) have been studied extensively in the last years[1-5]. Particularly, great attention was given to optical studies and Aharonov-Bohm (AB) effect in QRs[1,3]. Particularly, AB can occur in excitonic systems in which the charged carriers are confined and polarized in a cylindrical geometry[1]. The excitonic AB effect depends on the difference in relative rotation of electrons and holes that orbit the magnetic flux in a closed cylindrical geometry, and on the flux between them[1]. This effect results in an effective difference in phase of the carriers and in the observation of oscillations in photoluminescence (PL) energy and/or intensity[1]. Although the conventional AB effect is usually associated to charged systems, it has also been predicted for neutral excitons in QRs[1]. In this case, the applied magnetic field will modulate the PL of the system due to optical selection rules and the relative phase of these particles[1]. Therefore, the AB effect in neutral excitonic systems will also result in oscillations of PL peak position and PL intensity of QRs with increasing magnetic field[1]. In addition, it was also shown that these oscillations can be controlled by an external perpendicular electrical field[1].

Resonant tunneling diodes (RTDs) have also been a research focus for many years[6-23]. Several works investigated their fundamental physical properties and possible potential applications in spintronics[8-17]. For example, it was shown that spin polarization of carriers in RTDs can be voltage and light dependent under magnetic field[8-10]. Strong oscillations of circular polarization degree (CPD) were observed in RTDs under applied bias and high magnetic fields with maximum values around the resonant peak voltages[8]. In addition, it was evidenced the formation of highly spin-polarized two dimensional (2D) gases under high magnetic fields which are responsible for spin polarized injection of carriers into the quantum well (QW) of the RTDs[11].The formation of excitonic complexes in RTDs at hole and electron resonant tunneling condition was also demonstrated[12,18]. The physical properties of RTDs containing self-assembled InAs quantum dots (QDs) were also investigated[13-14,19-22]. It was shown that the spin polarization of an ensemble of QDs can also be voltage and light controlled due to the changes of charge state of QDs by an applied voltage, particularly at resonant tunneling condition[13-14]. However, there is no study of optical and spin properties of ensemble of InGaAs QRs in RTDs which could be an interesting system to evidence voltage controlled AB effects.

In this work, we have performed a systematic investigation of optical and spin properties of GaAs-AlGaAs RTDs containing a layer of InGaAs QRs in the QW region. We have measured the left and right circularly polarized PL at a temperature of 2 K from QRs and GaAs contact layers as a function of applied voltage under high magnetic fields up to 15 T. Under magnetic field, we have observed periodic oscillations of the QRs' PL intensity and the CPD with increasing applied voltage. This effect was explained by resonant tunneling effect and capture of carriers by an ensemble of QRs with different sizes.

SAMPLES AND EXPERIMENTAL SETUP

Our RTD devices were fabricated by molecular beam epitaxy on n+ (001) GaAs substrates. The device structure consists of two 8-nm-thick $Al_{0.4}Ga_{0.6}As$ tunnel barriers and a 10-nm thick GaAs QW, which contains a layer of InGaAs QRs. Undoped GaAs spacer layers with 50 nm width separate the barriers from

$2x10^{17}$ cm^{-3} n-doped GaAs layers of 50 nm width and 0.4 μm n+ Si doped GaAs layers[23]. Similarly, uncapped ring-shaped QD layers were prepared and investigated and revealed a QR density of $7x10^9$ cm^{-2} with lateral diameter of about 20 nm and a height of about 3 nm[23]. Typical AFM images of ring-shaped QD layers can be found in the reference [23]. The procedure used to obtain InGaAs ring-shaped QD structures and details of the samples were also described in reference [23].

The devices were processed into circular optical mesas with 400 μm diameter with annular AuGe electrical contacts. The optical excitation was given by a linearly polarized green line (532 nm) of a solid state laser. As a consequence, the photo-created carriers in RTD have not preferential spin polarization degree. Optical measurements were performed at low temperature (2 K) using a 0.5 m Andor spectrometer (wavelength resolution of 0.06 nm) with an electrically cooled InGaAs diode array. All measurements were performed under high magnetic field parallel to the tunnel current. Circularly-polarized right (σ^+) and left (σ^-) PL from the devices were selected with appropriate linear polarizer and quarter wave plate.

RESULTS AND DISCUSSION

Fig. 1(a) shows a schematic layer structure of a GaAs/AlGaAs RTD with InGaAs QRs inserted inside a GaAs QW. Fig. 1(b) shows schematically the potential profile of the RTD under applied voltage, light excitation and magnetic field parallel to the tunnel current. Under applied voltage, the majority electrons tunnel though the QW resonant states (labeled *E1, E2, E3)* which are formed by the combination of the residual InGaAs wetting layer potential and the GaAs QW[23]. For simplicity, the InGaAs wetting layer was not included in Fig.1. Photo-created holes are generated at the top contact region and can also tunnel resonantly through valence band QW confined states. In addition, carriers can also tunnel resonantly via higher energy confined states of different QRs. For simplicity, we have not shown all these levels in this diagram. These resonances were previously observed and reported in the literature[23]. Fig. 1(c) shows the current-voltage (I(V)) characteristics curve under dark and laser excitation at zero magnetic field. Under dark condition, we observed two electron resonances in the I(V) characteristics curve. The weak shoulder detected around 0.15 V (labeled E1) was associated to electron resonant tunneling into the lowest confined state of QW [23]. The strongest resonance was observed at 0.9 V which is associated to electron tunneling into the second QW subband labeled E2. Under laser excitation a large photocurrent is observed at lower voltages in the range of 0 - 0.4 V due to hole tunneling through the device. A hole resonant peak is also expected to be observed at low voltages due to resonant tunneling through hole confined state in the QW. However, we have only observed an additional structure in the I(V) curve under light excitation which was associated to the hole resonance .

Fig. 2(a) shows typical QRs' PL spectra obtained at zero magnetic field for different applied voltages. The PL spectra consist of four main peaks in the range of 1.1 - 1.3 eV. The physical origin of these PL spectra is due to different physical processes. The first process is associated to the direct photo-excitation and recombination in QRs. Under applied bias, another process can occur as carriers photo-created in the contacts can tunnel resonantly into the confined levels, and eventually they are captured by the QRs where they can recombine radiatively[21]. Actually, the typical capture time of carriers by QRs is ~ 1 ps, which is much shorter than the characteristic dwell times of electrons and holes which tunnel resonantly through the QW[21]. In addition, carriers can also tunnel through the confined states of QRs with different sizes and recombine radiatively in the lowest QRs states[23]. It was observed that the PL spectra shape of QRs does not present important dependence with the laser excitation power, which indicates that these different bands do not arise from higher energy levels in QRs[23]. Therefore, the PL features were associated to lower energy interband transitions from a multimodal distribution of QRs consisting of about four different sizes and/or composition[23]. We noted that the PL spectra are very sensitive to applied bias voltage. Fig. 2(b) shows the voltage dependence of the QRs PL intensity and the I(V) characteristics curve. Usually, the PL intensity and I(V) characteristics curve of RTDs are correlated as will be discussed below[10-11]. It was observed that the PL intensity increases with the increase of applied voltage up to about 0.4 V which corresponds to the voltage range that gives important photocurrent values. This result was associated to the hole resonant tunneling condition. The PL intensity depends on the hole and electron density of carriers in the QW region. In a simple model, the PL can be given by the product of the electron and hole density. It is well known that the carrier density in the QW increases with voltages associated to resonant tunneling condition[10-11]. Therefore, peaks of PL intensity are expected to be observed around the hole or electron resonance and therefore are correlated to the I(V) characteristics curve. In our case, we observed a PL intensity peak around 0.4 V and a small shoulder around 0.9 V. The small shoulder around 0.9

V was associated to the E2 resonance because there is a resonant peak E2 in the I(V) characteristics curve at this voltage. This shoulder is associated to the increase of electron density in the QW at the electron resonant tunneling condition. For higher applied bias the PL intensity is reduced due to the reduction of charge accumulated in the QW which reduces the carrier capture process by QRs and consequently reduces the PL intensity.

The PL intensity peak around 0.4 V is probably due to the increase of photogenerated hole density at the hole resonant condition. We have observed a structure in the I(V) characteristics curve which was associated to the hole resonant peak under light excitation which could explain the observed peak of PL intensity around 0.4 V.

Fig. 3(a) shows the polarization resolved PL from GaAs contact layers at 15 T. The contact PL spectra are very broad and clearly show the contribution of different emission bands: the excitonic transition from the undoped GaAs spacer layers (narrow peak at ~ 1.51 eV) and the recombination involving the n-doped GaAs layers (broad band). Both emissions are not expected to show changes in their peak energy with increasing applied bias voltage[11]. An additional PL emission peak was also observed at ~ 1.5 eV at B = 15 T. We will show below that this new peak is clearly voltage-dependent (Fig. 3(b)). This PL peak was associated to the recombination between confined electrons in the two-dimensional electron gas (2DEG) formed in the accumulation layer (Fig. 1(b)) and free tunneling holes[11] (labeled 2DEG-h). Fig. 3(b) shows the color code plot of polarization resolved PL intensity at B = 0 T and B = 15 T. It was observed that the contact PL intensity does not show important changes with applied bias except after E2 resonance where the optical recombination of

2DEG-h emerges[11]. It was observed that the 2DEG-h emission is highly circularly polarized. This result suggests that highly spin polarized carriers next to the barrier can inject highly spin polarized carriers[11] into the QRs which could increase the CPD .

Fig.4 shows typical polarization resolved PL spectra and the energy dependence of CPD of QRs under 0 V and 0.2 V. The energy dependence of the CPD was estimated by:

$$CPD = (I^{\sigma+} - I^{\sigma-})/(I^{\sigma+} + I^{\sigma-}) \qquad (1)$$

Where $I^{\sigma+}$ and $I^{\sigma-}$ are the intensity of $\sigma+$ and $\sigma-$ polarized emission.

It was observed that the polarization degree is higher for higher energies (where the emission due to smaller QRs. It was also observed that the polarization degree is higher under 0.2 V. This voltage corresponds to the hole resonant tunneling condition. Under 0 V, the polarization degree is associated to thermal occupation of spin states in the QRs. Under resonant tunneling condition, carriers tunnel through different spin states in the QW region and the polarization degree is increased as expected[11].

Fig. 5 shows the color-coded maps for QRs emission under 0 T and 15 T, and T= 2 K. We observed that the QR PL intensity is higher at low voltages and decreases for higher voltages. Changes in PL spectra were observed such as the intensity and linewidth variations with applied bias voltage. These changes cannot be correlated to resonant tunneling peaks observed in the I(V) characteristics curve. However, small structures were observed in the I(V) curve of other diodes for the same RTD[23] and were associated to excited states of

QRs[23]. Therefore we associated these changes to resonant tunneling through excited states of QRs.

Fig. 6 shows the voltage dependence of PL intensity and CPD of QRs under 15T. The CPD was obtained by the integrated PL intensity of the total PL spectra of QRs. Therefore, the polarization degree is due to the contribution of all different bands associated to QRs with different sizes. The PL intensity and polarization degree show periodic oscillations with applied bias voltages. The QRs polarization degree reaches a maximum modulus value of ~ 30% around ~ 0.2 V. We would like to emphasize that these oscillations are only observed for RTDs with QRs. We have also investigated the voltage dependence of RTD with InAs QDs[13,14]. For RTDs with QDs the polarization degree is also higher at low voltages and decreases with increase applied bias. However, no oscillations of CPD were observed with applied bias voltage for RTDs with QDs. The voltage dependence of CPD for InAs QDs was previously associated to the formation of excitonic complexes around hole and electron resonant tunneling condition. In our case, there is no evidence of formation of excitonic complexes with applied voltage in RTDs with QRs. These oscillations of PL intensity and polarization degree were associated to resonant tunneling to excited states of QRs in agreement of a previous work carried out on this device[23].

We have also investigated the magnetic field dependence of intensity and CPD of PL spectra of QRs. As it was discussed in the introduction, it was expected to observe oscillations and voltage control of these oscillations of PL intensity and polarization degree with magnetic field due to AB effect. However, we have not observed any evidence of the AB effect in the magnetic dependence of both PL intensity (not shown here) and polarization degree,

Figure 7 shows the magnetic field dependence of CPD for the ensemble of QRs. The polarization degree increases with the increase of magnetic field and we have no evidence of oscillations. Therefore, it is very difficult to associate our results to the AB effect.

CONCLUSION

We have investigated the magneto-transport and polarization-resolved PL under linearly polarized laser excitation from an ensemble of InGaAs QRs incorporated in GaAs/AlGaAs RTDs as function of applied voltage. Under magnetic field, the PL intensity and the spin polarization degree of the QRs shows periodic oscillations with applied bias voltage. These oscillations were associated to resonant tunneling to excited states of QRs in agreement of a previous experiment performed on this device[23]. It was found that the QRs polarization degree presents a maximum value (~ -30% at B = 15 T) around the hole resonant tunneling condition. In addition, there is no evidence of the AB effect in the RTDs with InGaAs QRs. Our results could be useful for voltage control of spin properties of QRs incorporated in RTDs and for the possible design of semiconductor devices containing QRs.

ACKNOWLEDGMENTS

The authors acknowledge the financial supports from the Brazilian agencies Fundação de Amparo a Pesquisa do Estado de São Paulo (grants FAPESP 2012/24055-6 and 2016/07239-7), Coordenação de Aperfeiçoamento de Pessoal de Nível Superior / PVE (CAPES) and Conselho Nacional de

Desenvolvimento Científico e Tecnológico (CNPq) and the UK Engineering and Physical Sciences Research Council.

REFERENCES

1. V. M. Fomin, *Physics of Quantum Rings*. (Springer-Verlag Berlin Heidelberg, 2014).

2. Y. Huang, Y. Puttisong, I. A. Buyanova, W. M. Chen. *Nano Research.* 9, 602 (2016).

3. F. Ding, N. Akopian, B. Li, U. Perinetti, A. Govorov, F. M. Peeters, C. C. Bof Bufon, C. Deneke, Y. H. Chen, A. Rastelli, O. G. Schmidt and V. Zwiller, *Phys. Rev. B.* 82, 075309 (2010).

4. K. Mukai, *J. Nanosci. Nanotechnol*. 14, 2148 (2014).

5. C. Kloeffel, D. Loss, *Annu. Rev. Condens. Matter Phys.* 4, 51 (2013).

6. H. Mizuta , T. Tanoue, *The Physics and Application of Resonant Tunnelling Diodes* (Cambridge University Press, Cambridge, 1995).

7. Y. G. Gobato, J. M. Berroir, Y. Guldner , J. P. Vieren, F. Chevoir, B. Vinter, *Phys. Rev. B.* 44, 13795 (1991).

8. H. B. de Carvalho, M. J. S.P. Brasil, Y. Galvão Gobato, G. E. Marques, H. V. A. Galeti, M. Henini, G. Hill, *Appl. Phys. Lett.* 90, 62120 (2007).

9. L. F. dos Santos, Y. Galvão Gobato, G. E. Marques, M. J. S. P. Brasil, M. Henini, R. Airey, *Appl. Phys. Lett.* 91, 073520 (2007).

10. L. F. dos Santos, Y. Galvão Gobato, G. E. Marques, M. J. S. P. Brasil, M. Henini, R. Airey, *Appl. Phys. Lett.* 92, 143505 (2008).

11. Y. Galvão Gobato, H. V. A. Galeti, L. F. dos Santos, V. López-Richard, D. F. Cesar, G. E. Marques, M. J. S. P. Brasil, M. Orlita, J. Kunc, D. K. Maude, M. Henini, R. J. Airey, *Appl. Phys. Lett.* 99, 233507 (2011)

12. A. Vercik, Y. Galvão Gobato, M. J. S. P. Brasil, *J. Appl. Phys.* 92, 1888 (2002).

13. E. C. dos Santos, Y. Galvão Gobato, M. J. S. P. Brasil, D. A. Taylor, M. Henini, *Nanoscale Res. Lett.* 6, 115 (2011).

14. J. Araujo e Nobrega, V. Orsi Gordo, H. V. A. Galeti, Y. Galvão Gobato, M. J. S. P. Brasil, D.Taylor, M. Orlita, M. Henini, *Superlat. Microst.* 88, 574 (2015).

15. A. Slobodskyy, C. Gould, T. Slobodskyy , C. R. Becker, G. Schmidt, L. W. Molenkamp, *Phys. Rev. Lett.* 90, 246601 (2003).

16. H. B. de Carvalho, M. J. S. P. Brasil, V. Lopez-Richard, Y. Galvão Gobato, G. E. Marques, I. Camps, L. C. O. Dacal, M. Henini, L. Eaves, G. Hill, *Phys. Rev. B.* 74, 041305 (2006).

17. M. Ruth, C. Gould, L. W. Molenkamp, *Phys. Rev. B.* 83,155408 (2011).

18. F. J. Teran, L. Eaves, L. Mansouri, H. Buhmann, D. K. Maude, M. Potemski, M. Henini , G. Hill, *Phys. Rev. B.* 71, 161309 (2005).

19. A. Patanè, A. Polimeni, L. Eaves, P. C. Main, M. Henini, Yu V. Dubrovskii, A. E. Belyaev, P. N. Brounkov, E. E. Vdovin, Yu N. Khanin , and G. Hill*, J. Appl. Phys.* 88, 2005 (2000).

20. A. Polimeni, M. Henini, A. Patane, L. Eaves , P. C. Main, *Appl. Phys. Lett***.** 73, 1415 (1998).

21. A. Patane, R. J. A. Hill, L. Eaves, P. C. Main, M. Henini, M. L. Zambrano, A. Levin, N. Mori, C. Hamaguchi, Y. V. Dubrovskii, E. E. Vdovin, D. G. Austing, S. Tarucha, G. Hill, *Phys. Rev. B.* 65, 165308 (2002).

22. A. Patane, P. C. Main, L. Eaves, A. Levin, M. Henini, G. Hill, *Physica E* 13, 170 (2002).

23. F. Pulizzi, D. Walker, A. Patanè, L. Eaves, M. Henini, D. Granados, J. M. Garcia, V. V. Rudenkov, P. C. M. Christianen, J. C. Maan, P. Offermans, P. M. Koenraad, G. Hill , *Phys. Rev. B*. 72, 085309 (2005).

FIGURE CAPTIONS

Fig.1: (a) A schematic layer structure of a GaAs/AlGaAs RTD with InGaAs QRs (b) Schematic conduction and valence band diagram of the device containing InGaAs QRs under applied bias, optical excitation and magnetic field. For simplicity, the InGaAs wetting layer was not included; (c) I(V) characteristics curve at 2 K and 0 T under dark and laser excitation.

Fig 2: (a) Typical PL spectra from QRs for different applied voltages under B = 0 T and T = 2 K; (b) InGaAs QRs PL integrated intensity as function of applied bias voltage.

Fig.3: (a) Typical polarized resolved PL spectra from GaAs contact layers at 15 T and 2 K; Color coded maps of polarized resolved PL intensities from GaAs contact as a function of applied voltage under (b) 0T and 15T for (c) σ+ and (d) σ- emission at 2K.

Fig.4: QRs' PL spectra under 15 T and 2 K for 0 V and 0.2 V.

Fig. 5: Color-coded maps of polarization resolved PL intensities of QRs as a function of voltage under (a) 0 T and 15T for (b) σ+ and (c) σ- PL at 2 K.

Fig. 6: (a) Voltage dependence of integrated PL intensity and the modulus of CPD of the ensemble of QRs. (b) Modulus of CPD versus applied bias voltage.

Fig 7: Magnetic field dependence of CPD for the ensemble of QRs for 0 and 0.4 V under B = 15 T and T = 2 K.

Figure 1

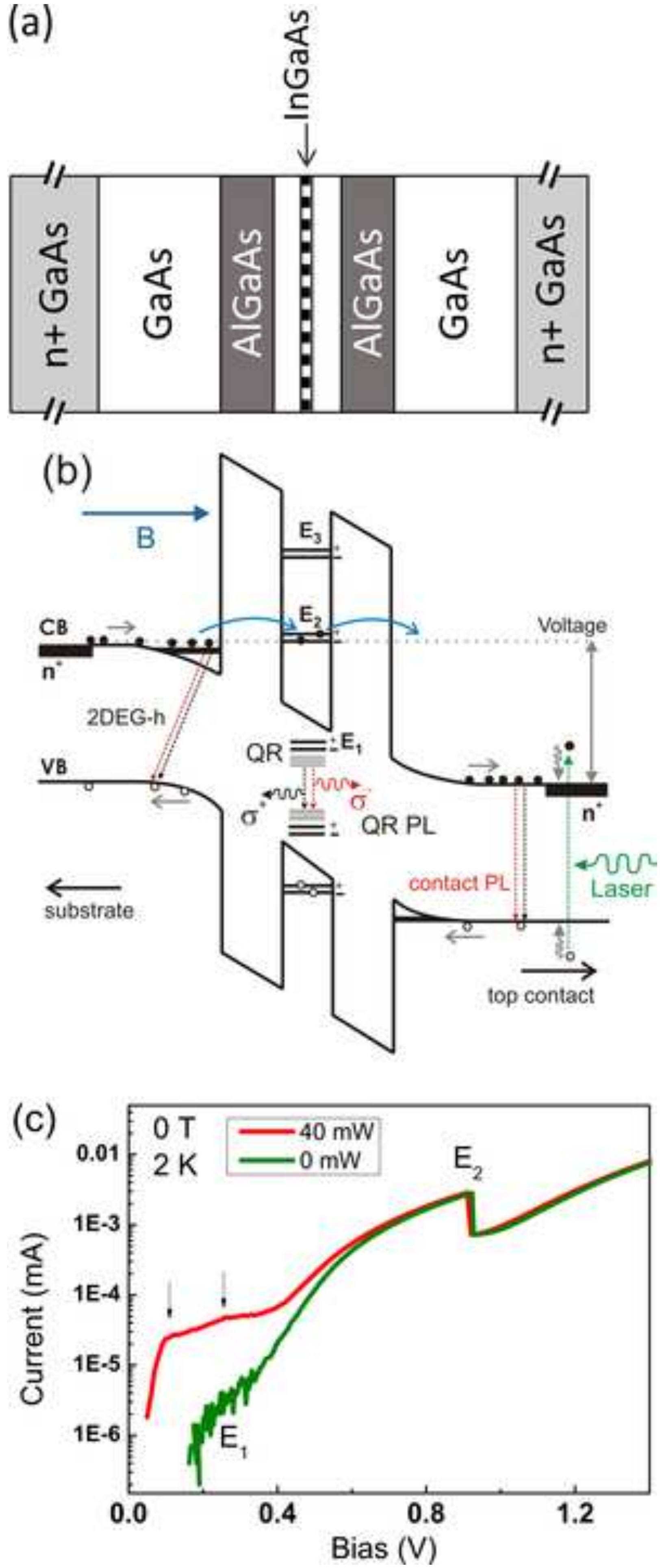
(a)
InGaAs
n+ GaAs
GaAs
AlGaAs
AlGaAs
GaAs
n+ GaAs
(b)
B
E3
E2
E1
CB
n+
Voltage
2DEG-h
VB
QR
QR PL
σ+
σ-
n+
contact PL
Laser
substrate
top contact
(c)
0 T
2 K
40 mW
0 mW
E2
E1
Current (mA)
Bias (V)
0.01
1E-3
1E-4
1E-5
1E-6
0.0
0.4
0.8
1.2

Figure 3

Click here to download Figure Figure 3.TIF

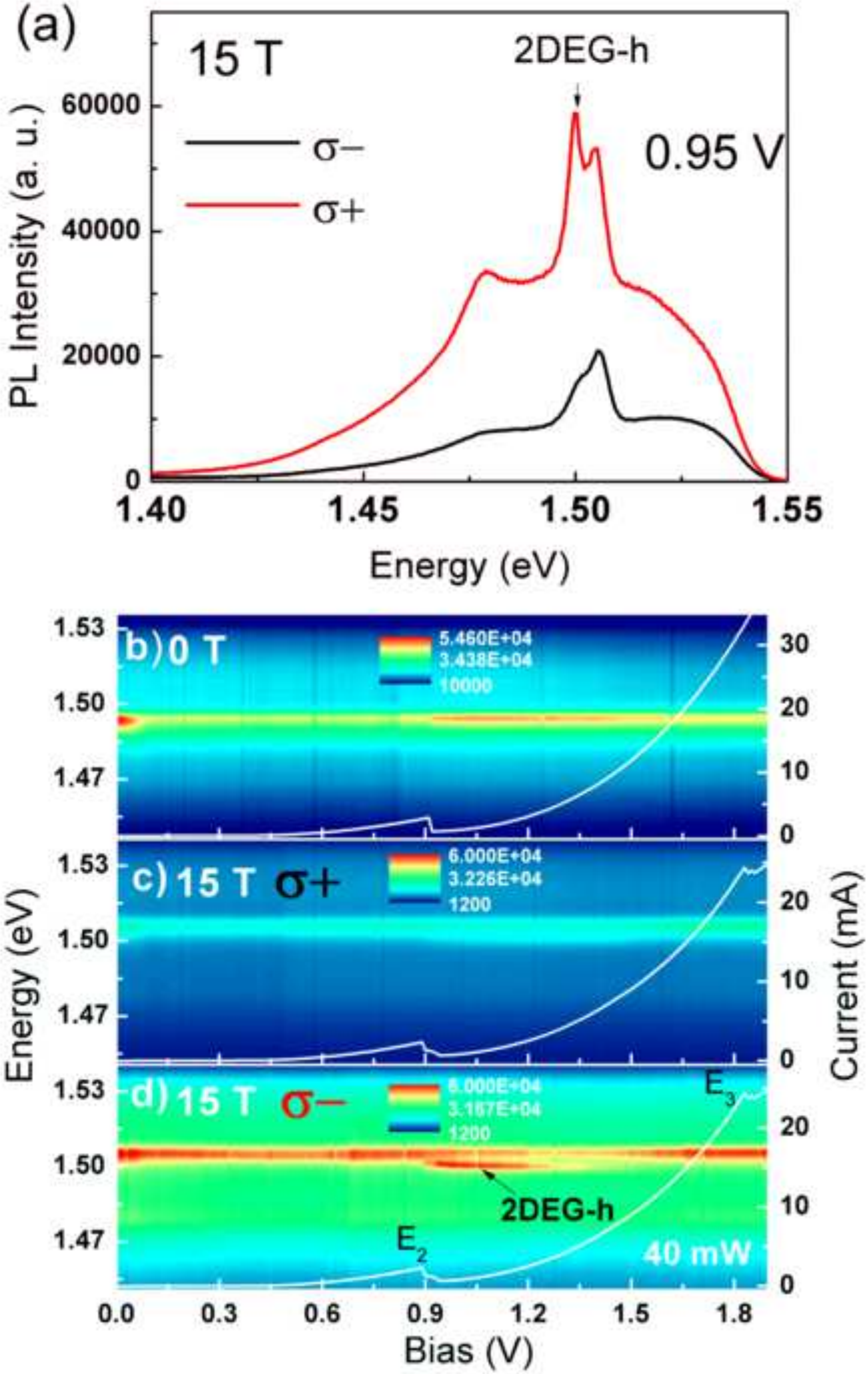

Figure 4

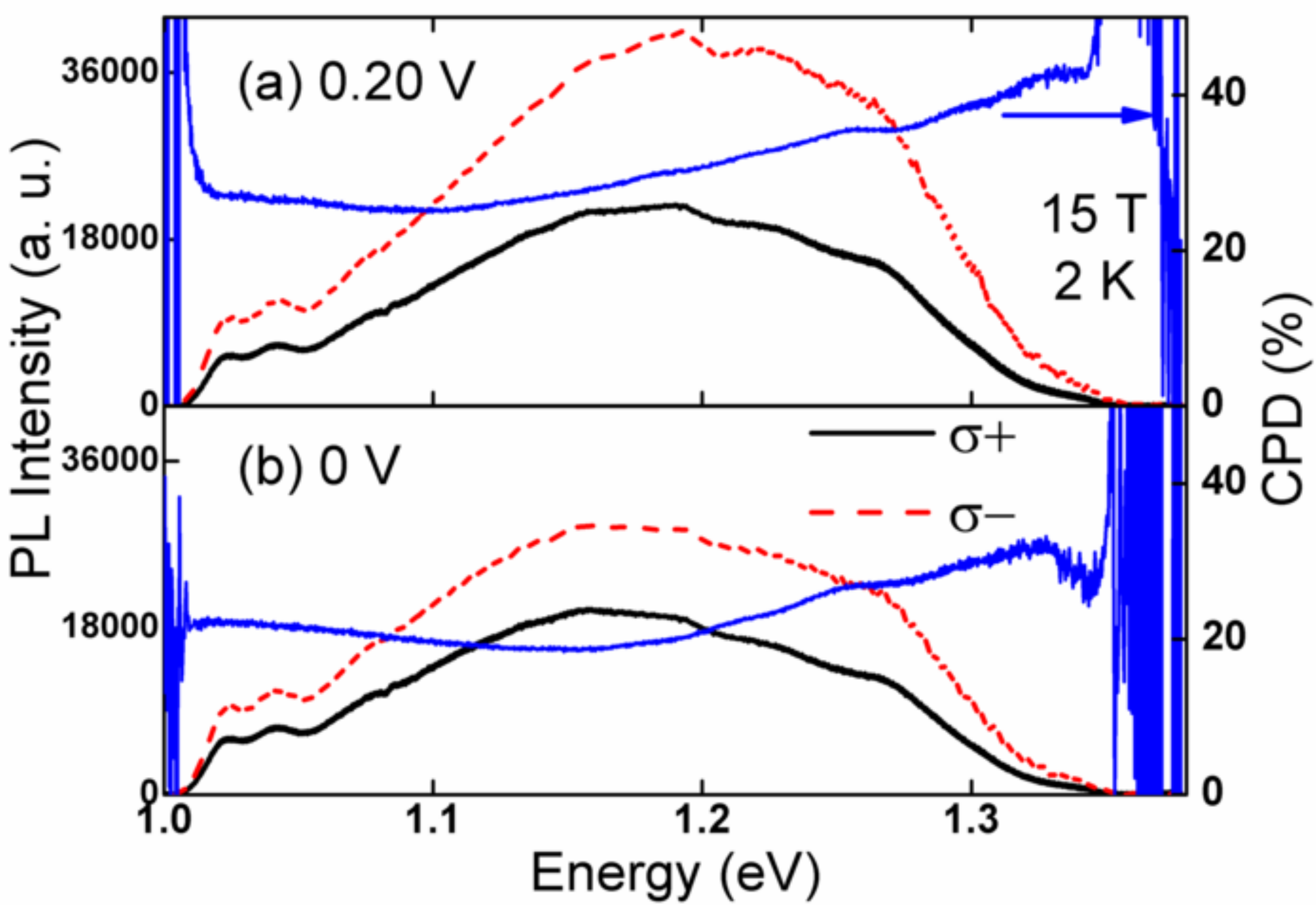
(a) 0.20 V
(b) 0 V
15 T
2 K
σ+
σ−
PL Intensity (a. u.)
CPD (%)
Energy (eV)
36000
18000
0
40
20
1.0
1.1
1.2
1.3

Figure 5

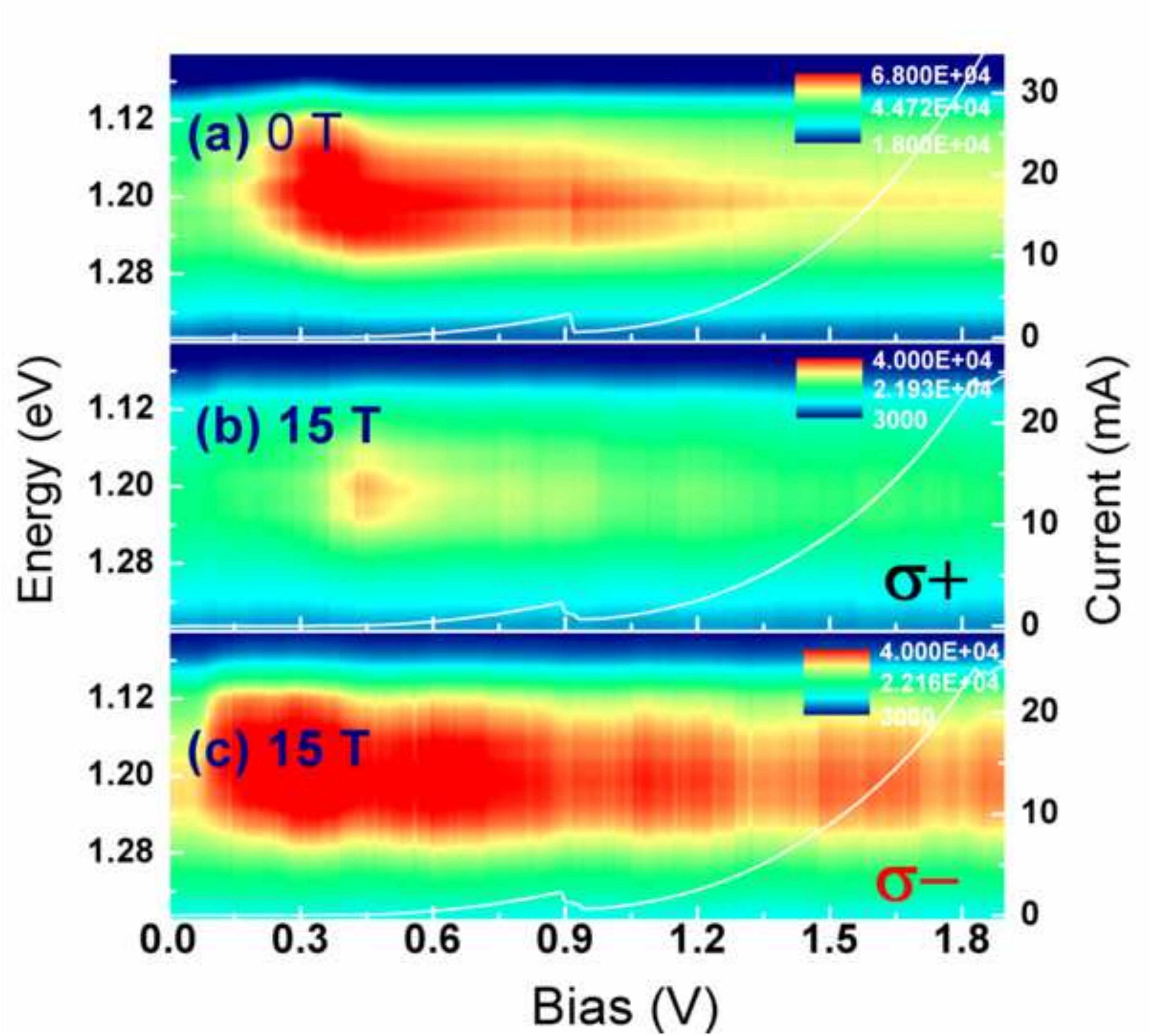

(a) 0 T
6.800E+04
4.472E+04
1.800E+04
(b) 15 T
4.000E+04
2.193E+04
3000
σ+
(c) 15 T
4.000E+04
2.216E+04
3000
σ−
1.12
1.20
1.28
Energy (eV)
Current (mA)
30
20
10
0
0.0
0.3
0.6
0.9
1.2
1.5
1.8
Bias (V)

Figure 6

Click here to download Figure Figure 6.tif

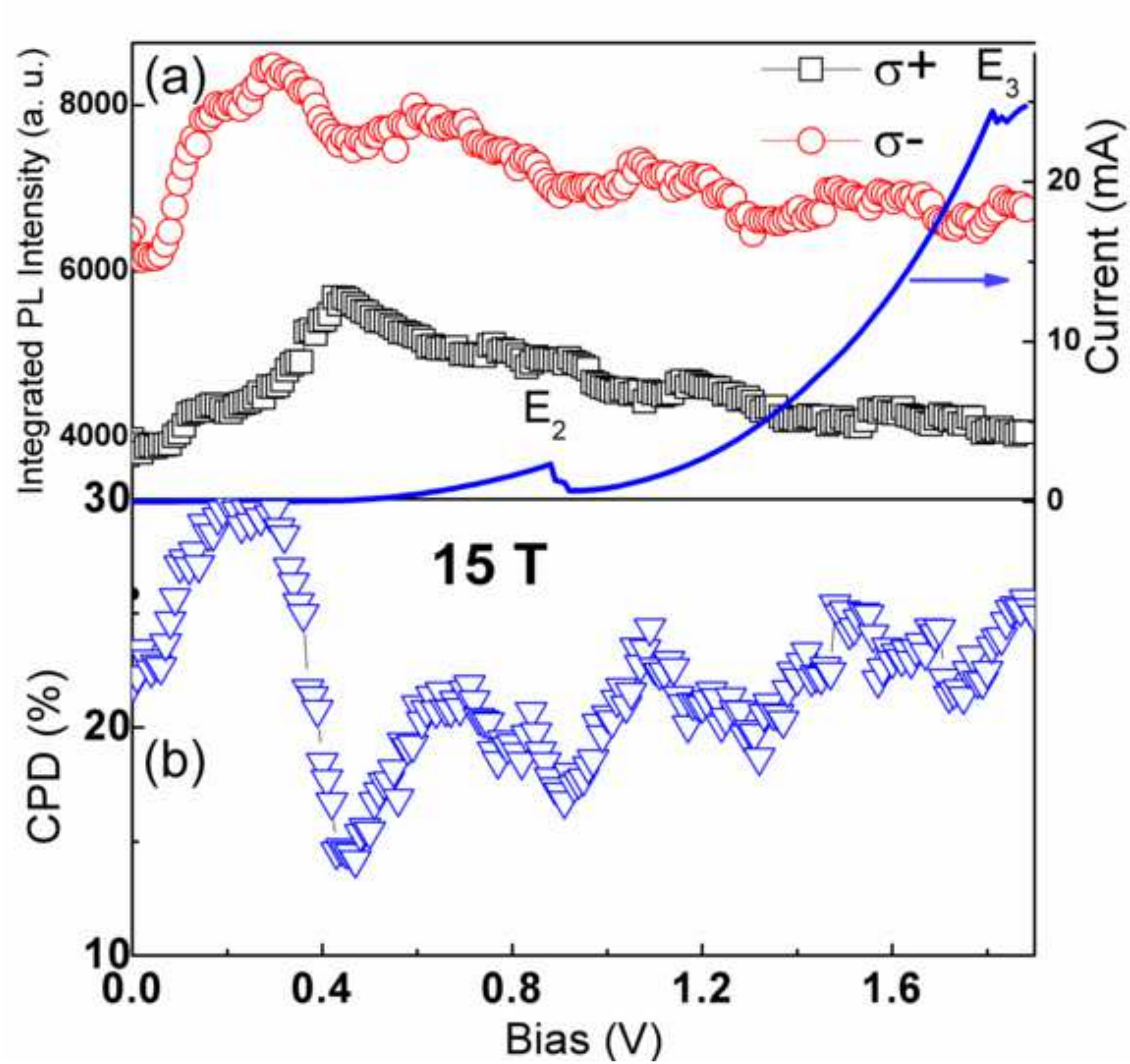

Figure 7

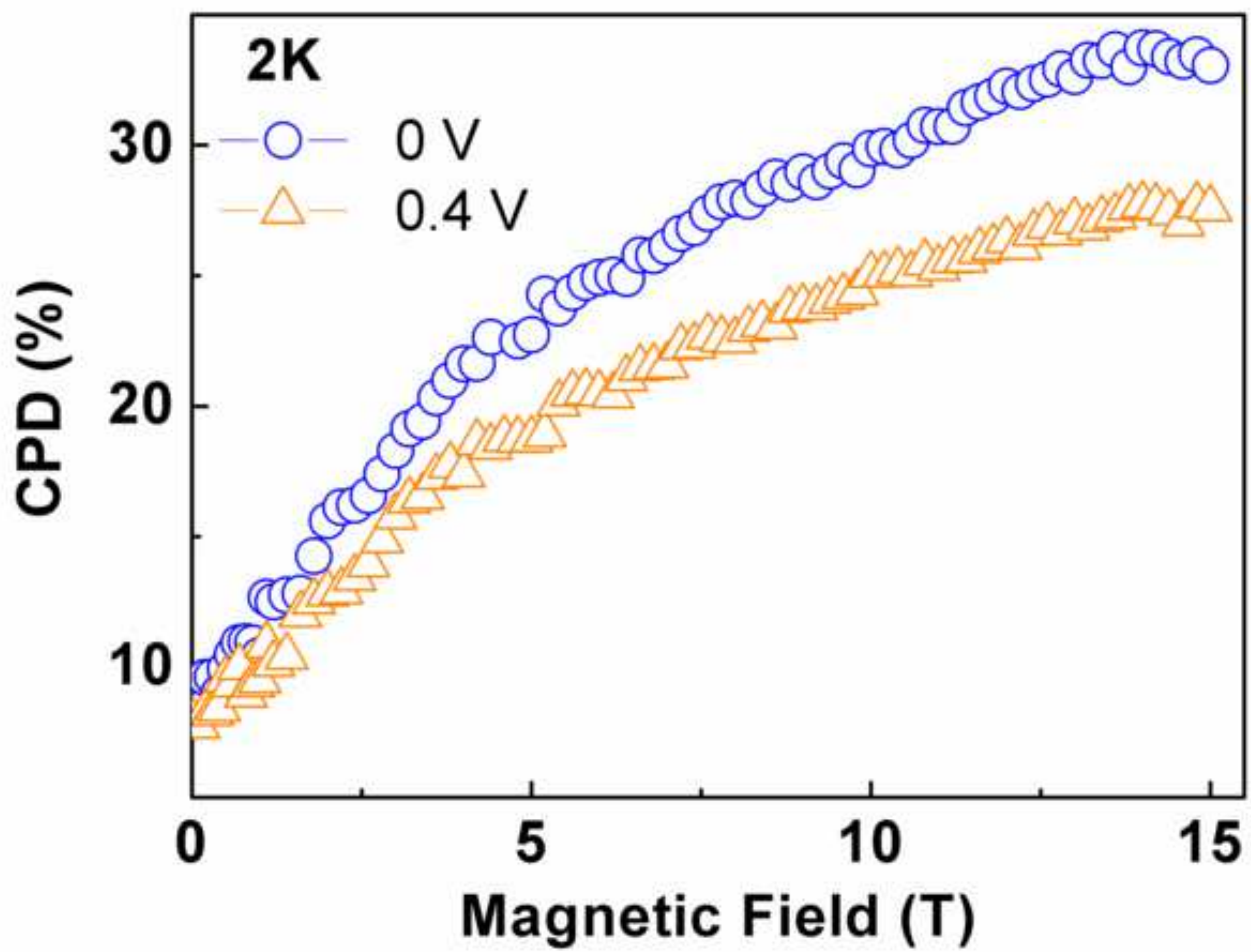

Figure

Click here to download Figure Fig2_new.tif